From perfect to fractal transmission in spin chains

Gabriele De Chiara, Davide Rossini, Simone Montangero, and Rosario Fazio

NEST–INFM & Scuola Normale Superiore, Piazza dei Cavalieri 7, I-56126 Pisa, Italy[*]
(Received 23 February 2005; published 20 July 2005)

Perfect state transfer is possible in modulated spin chains [Phys. Rev. Lett. **92**, 187902 (2004)], imperfections, however, are likely to corrupt the state transfer. We study the robustness of this quantum communication protocol in the presence of disorder both in the exchange couplings between the spins and in the local magnetic field. The degradation of the fidelity can be suitably expressed, as a function of the level of imperfection and the length of the chain, in a scaling form. In addition the time signal of fidelity becomes fractal. We further characterize the state transfer by analyzing the spectral properties of the Hamiltonian of the spin chain.

PACS number(s): 03.67.Hk, 03.67.Pp, 05.50.+q

I. INTRODUCTION

The ability to transfer a quantum state between distant parties is one of the basic requirements in many quantum information protocols, we mention for example quantum key distribution [1] or teleportation [2]. A very successful area where the implementation of quantum state transmission has been realized is quantum optics. The carriers of information (photons) can be addressed and transmitted with high control and with a low level of decoherence. Very recently, in view of the great potentialities of solid-state quantum information, attention is also focusing on the problem of the transfer of quantum information in a solid-state environment. A possible way to follow would be to properly design couplings between optical and solid-state systems [3]. Alternatively one could also think to realize quantum channels using condensed-matter systems. In Ref. [4] Bose has shown that a Heisenberg spin chain is able to act as a quantum channel over reasonable distance ($\sim 10^2$ lattice sites). Information capacities for this Heisenberg channel have been analyzed in Ref. [5]. In Ref. [6] a slightly different scheme has been proposed, in which the simple spin chain has been replaced with an isotropic antiferromagnetic spin ladder. A great advantage of these approaches is that state transfer occurs due to the interaction between the spins of the chain and no dynamical control is required (except for the preparation and the detection of the state). Proposals to implement this scheme with superconducting nanocircuits [7,8] have been already put forward and very likely these implementations can also be extended to other solid-state systems.

Perfect transfer can be achieved over arbitrary distances in spin chains under many different hypotheses: by a proper choice of the modulation of the coupling strengths as suggested [9], if local measurements on the individual spins can be implemented [10], when communicating parties have access to limited numbers of qubits in a spin ring [11] or by using several spin chains in parallel [12]. As in all situations in quantum information, the efficiency of such protocols relies on the capability of isolating the experimental setup from the external world (decoherence), and on the possibility to reduce all possible static imperfections [13,14]. In the case of the protocols presented in Refs. [4,9], where no control is needed on the system during the state transfer, that is, no dynamical control is applied, the coupling to the environment is supposed to be weak. It thus remains to be seen how the quantum channel is robust against static imperfections which would be unavoidable (especially in solid-state implementations with engineered nanodevices). Particularly important to consider is the case when, in the ideal case, perfect state transfer is obtained.

In this paper we address the problem of the effects of static imperfections on the protocol presented in Ref. [9], which has already been experimentally implemented in Ref. [15] using a three qubit nuclear magnetic-resonance quantum computer. We study the sensitivity of the state transfer to random variations both of the coupling between the spins and of an externally applied magnetic field. In view of the possible applications with solid-state systems, also the case of correlated disorder will be considered. Similar questions for quantum computation protocols have been already analyzed in Refs. [13,14]. In that case the loss of efficiency of the protocol was related to the appearance of quantum chaos in a quantum computer register. This relation has been characterized studying the level spacing statistics. Following these lines we study the transition of the level spacing statistics of the spin chain in the presence of static imperfections. Even though it is not possible to frame this problem with the random matrix theory [16], we show that the level spacing statistic is still a convenient tool to describe the system efficiency in performing the state transfer.

The presence of static imperfections leads to another clear signature of the modified properties of the spectrum in the fidelity. The degradation of the state transfer corresponds to the emergence of a fractal signal, i.e., the fidelity changes from a periodic function of time to a fractal time series. This behavior has the same origin as the one found in the probability densities of the quantum evolution in tight-binding lattices [17,18].

The paper is organized as follows. In Sec. II we introduce the model used throughout this work, we set up the notations, and we briefly review the quantum state transmission protocol of Refs. [4,9]. We then analyze the fidelity of the transferred state (Sec. III), and the level spacing statistics of the Hamiltonian of the system (Sec. IV). Interestingly, the dependence of the fidelity, as a function of the length of the chain and the level of disorder, obeys simple scaling laws. In Sec. V we take a closer look at the behavior of the fidelity as a function of time. The presence of static imperfections leads

to a fractal behavior of the time signal of the fidelity. In the same section, we relate the fractal dimension to the amount of disorder present in the chain. The last section is devoted to the conclusions.

II. MODEL

The protocol introduced in Ref. [4] enables quantum state transfer between two parties by means of a spin chain: The state of the left-most qubit is transferred to the right-most qubit after a given time (dictated by the dynamics of the chain). In Ref. [9] the approach is the same as in Ref. [4], the idea is to use a modulated chain whose Hamiltonian is given by

$$H = \sum_{k=1}^{N} B_k \sigma_k^z + \sum_{k=1}^{N-1} J_k (\sigma_k^x \sigma_{k+1}^x + \sigma_k^y \sigma_{k+1}^y). \tag{1}$$

In Eq. (1) N is the number of spins in the chain, σ_k^x, σ_k^y, σ_k^z are the Pauli operators of the kth spin. The parameters B_k and J_k are, respectively, the local magnetic field and the exchange coupling constant. Both couplings depend on the position of the site (or of the link) on the chain. In order to achieve perfect state transfer, the system parameters are chosen to be

$$B_k = 0, \quad J_k = J\sqrt{k(N-k)}.$$

The spin chain is initially (at time $t=0$) prepared in the state

$$|\Psi_0(\vartheta,\varphi)\rangle = (\cos\vartheta|0\rangle + \sin\vartheta\, e^{i\varphi}|1\rangle) \otimes |0\rangle^{\otimes(N-1)}, \tag{2}$$

that is, the left-most spin is prepared in a given superposition of its two levels while the others are in their ground state. The state (2) will evolve accordingly to the dynamics dictated by Eq. (1). Since the Hamiltonian commutes with the total spin component along the z direction, the relevant sector of the Hilbert space is spanned by the states

$$|j\rangle \equiv |0,0,\ldots0,1,0,\ldots0\rangle, \tag{3}$$

which for $j=1,\ldots,N$ represents a state of the chain where the jth spin is prepared in $|1\rangle$ and the other $N-1$ ones in $|0\rangle$. The global state of the chain at time t is

$$|\Psi(t)\rangle = \cos\vartheta|0\rangle + \sin\vartheta e^{i\varphi}\sum_{j=1}^{N} f_j(t)|j\rangle, \tag{4}$$

where $|0\rangle$ is the chain state with all the spins in $|0\rangle$ and where (we set $\hbar=1$)

$$f_j(t) \equiv \langle j|e^{-iHt}|1\rangle. \tag{5}$$

The accuracy of the state transfer is determined through the analysis of the fidelity

$$\mathcal{F}(t,\vartheta,\varphi) = \langle\Psi_0(\vartheta,\varphi)|\rho_N(t)|\Psi_0(\vartheta,\varphi)\rangle$$

where $\rho_N(t)$ is the reduced density matrix of the Nth spin at time t. We consider the fidelity averaged over the initial state $|\Psi_0\rangle$ distributed uniformly over the Bloch sphere [4],

$$\mathcal{F}(t) = \langle\mathcal{F}(t,\vartheta,\varphi)\rangle_{\vartheta,\varphi} = \frac{|f_N|}{3} + \frac{|f_N|^2}{6} + \frac{1}{2}. \tag{6}$$

We ignore the phase of f_N as it can be gauged away by a proper choice of the external field. Eventually, we will aver-
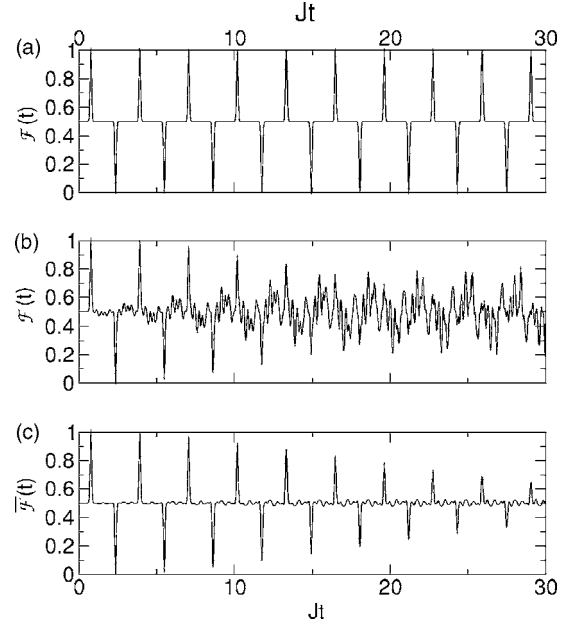

FIG. 1. Fidelity of the Nth spin with $N=100$ as a function of time. (a) Without imperfections, $\varepsilon_J=\varepsilon_B=0$. (b) With imperfections $\varepsilon_J=10^{-2}$, $\varepsilon_B=0$, $N_{av}=1$. (c) With imperfections $\varepsilon_J=10^{-2}$, $\varepsilon_B=0$ averaged over $N_{av}=10^2$ realizations.

age over different disorder realizations, that is,

$$\bar{\mathcal{F}}(t) = \langle\mathcal{F}(t)\rangle_{\mathcal{D}}, \tag{7}$$

where $\langle\cdot\rangle_{\mathcal{D}}$ stands for the average over different imperfection configurations. In Ref. [9] it has been shown that after a time $t_n=(2n+1)\pi/4J$ (n integer) the state of the left-most spin is transferred exactly to the right-most spin. This is due to the fact that the Hamiltonian (2) can be viewed as that of a pseudospin $\vec{S}=(N-1)/2$ that precesses in a constant magnetic field. The state transmission is equivalent to a π rotation of the spin. In order to analyze the robustness of this protocol to static imperfections, we model their effects by adding to the Hamiltonian a random perturbation both in the exchange couplings and in the local variations of the magnetic field. The coefficients in Eq. (1) are replaced with the new values

$$B_k \rightarrow b_k, \quad J_k \rightarrow J_k(1+\delta_k),$$

where δ_k and b_k are random variables with uniform distribution in the intervals $\delta_k \in [-\varepsilon_J, \varepsilon_J]$ and $b_k \in [-\varepsilon_B, \varepsilon_B]$. The results presented in this paper are obtained by averaging over N_{av} different disorder realizations.

III. STABILITY OF THE COMMUNICATION IN A DISORDERED CHAIN

We numerically solve the Schrödinger equation for the dynamical evolution and compute the fidelity of the right-most spin with respect to the input state. In Fig. 1 we plot typical results of this evolution both for the ideal case [Fig. 1(a)] and in presence of imperfections [Fig. 1(b)]. Figure 1(c) is the result of an average over different disorder real-
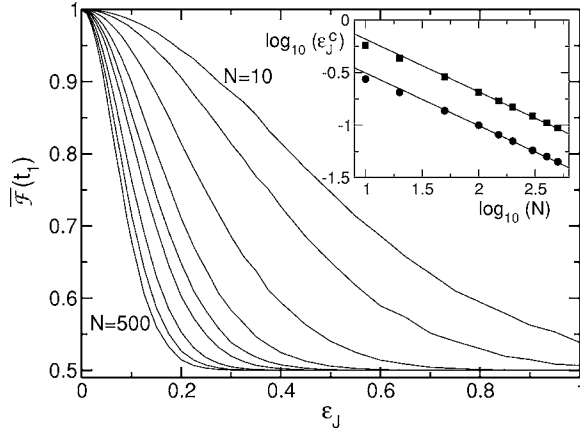
FIG. 2. Averaged fidelity at time t_1 as a function of the disorder ε_J for different spin chain lengths and $\varepsilon_B=0$, $N_{av}=10^3$. From right to left, $N=10, 20, 50, 100, 150, 200, 300, 400, 500$. Inset: ε_J^c as a function of N obtained from the condition $\bar{\mathcal{F}}(t_1)=0.9$ (circles) and $\bar{\mathcal{F}}(t_1)=0.7$ (squares). Straight lines are proportional to $N^{-0.5}$. Here and in the following figures the logarithms are decimal.
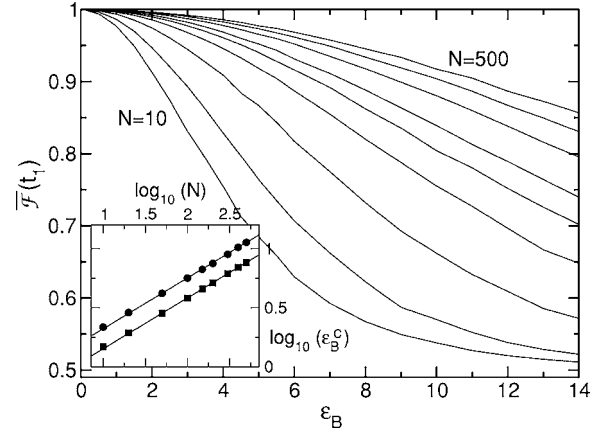

FIG. 3. Averaged fidelity at time t_1 as a function of magnetic field disorder ε_B for different spin-chain lengths and $\varepsilon_J=0$, $N_{av}=10^3$. From left to right $N=10, 20, 50, 100, 150, 200, 300, 400, 500$. Inset: ε_B^c as a function of N obtained from the condition $\bar{\mathcal{F}}(t_1)=0.9$ (circles) and $\bar{\mathcal{F}}(t_1)=0.95$ (squares). Straight lines are proportional to $N^{0.43}$.

izations. In the presence of disorder the simple periodicity of the fidelity oscillation is lost. Moreover, the maximal value of the fidelity is less than unity (it is reached at slightly different time intervals as compared to the ideal case). Thus the optimal time for state transfer should be inferred for each experimental sample. The original (in the ideal case) periodicity of the signal is recovered averaging over different disorder realizations, however, the maxima are progressively suppressed on increasing time. Therefore the optimal state transfer, in presence of imperfections, is obtained in correspondence of the first peak at time $t_1=\pi/4J$.

In this section we concentrate on the dependence of the optimal fidelity ($\bar{\mathcal{F}}$ at time t_1) as a function of static imperfection strength and of the chain length.

In Fig. 2 we report the fidelity as a function of ε_J for different chain lengths assuming, for the moment, that there is no disorder in the local field ($\varepsilon_B=0$). The opposite situation, with disordered local magnetic field ($\varepsilon_B\neq0$) and ideal nearest-neighbor interaction ($\varepsilon_J=0$) is shown in Fig. 3. These sources of disorder lead to a striking different behavior. While in the first case the error introduced by the imperfections increases with N, the effect of the disorder on local magnetic field decreases, becoming less effective on increasing the chain length. For completeness we show the case where both ε_B and ε_J are different from zero in Fig. 4. The fact that the two effects are almost independent can be traced back to the fact that we are working in the sector with one spin up.

The behavior of the fidelity obeys a simple scaling law. We verified numerically that the fidelity scales as

$$\bar{\mathcal{F}}(t_1) = \frac{1}{2}(1 + e^{-\kappa_J N \varepsilon_J^2 - \kappa_B \varepsilon_B^2/N}), \qquad (8)$$

where $\kappa_J \sim 0.2$ and $\kappa_B \sim 0.7$. The constants κ_J (κ_B) have been obtained from the dependence, as a function of N, of the

value ε_J^c (ε_B^c) at which the fidelity reaches a given threshold value (see the insets of Figs. 2 and 3).

The scaling given in Eq. (8) can be justified in the limit of very small disorder by means of perturbation theory. In the limit $\varepsilon_J t$, $\varepsilon_B t \ll 1$, the fidelity reads

$$\bar{\mathcal{F}}(t) \approx 1 - \frac{\varepsilon_B^2}{3}\sum_{k=1}^{N} \{2\,\mathrm{Re}[D_{k,k}(t)] - C_k^2(t)\}/3$$

$$- \frac{\varepsilon_J^2}{3}\sum_{k=1}^{N} \{2\,\mathrm{Re}[F_{k,k}(t)] - E_k^2(t)\}/3. \qquad (9)$$

The coefficients C_k, $D_{k,k}$, E_k, and $F_{k,k}$ as well as the details of the calculation are given in the Appendix. The disorder in the local magnetic field averages out in the limit of infinite spin chains. In view of the little effect of random fields on the quantum communication over long chains, from now on we
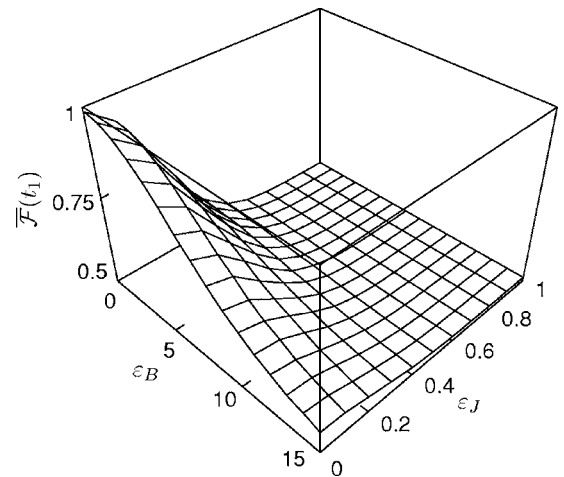

FIG. 4. Average fidelity at time t_1 as a function of the amplitudes of disorder ε_J, ε_B for a $N=50$ spin network, $N_{av}=100$.
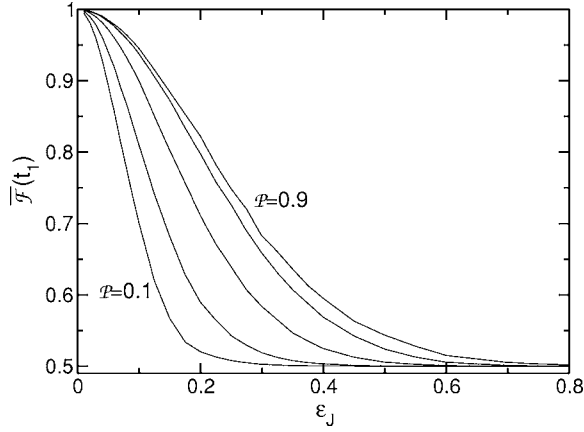
FIG. 5. Fidelity at time t_1 as a function of ε_J with $N=100$, $N_{av}=200$ and from left to right $\mathcal{P}=0.1$, 0.25, 0.5, 0.75, 0.9.

FIG. 6. Level spacing statistics $P(s)$ for $N=100$, $\epsilon_B=0$, $N_{av}=10^3$ and different values of ϵ_J: $\epsilon_J=10^{-3}$ (circles), $\epsilon_J=2\times10^{-2}$ (squares), $\epsilon_J=5\times10^{-2}$ (diamonds), $\epsilon_J=2\times10^{-1}$ (triangles up), $\epsilon_J=1$ (triangles down). Inset: magnification of the same figure around $s=1$. The dashed line corresponds to the Poissonian $P_P(s)$.

will consider only the effect of disordered exchange coupling between spins.

The presence of spatial correlation in the disorder is a concrete possibility in experimental realizations of this protocol, as, for example, with Josephson-junction chains [7,8]. We model correlated disorder as follows: The sign of any single δ_k, the error on the kth coupling, is correlated with the previous one following the rule

$$\delta_i\delta_{i-1}>0 \quad \text{with probability } \mathcal{P},$$

$$\delta_i\delta_{i-1}<0 \quad \text{otherwise.} \tag{10}$$

The correlations introduced in Eq. (10) result in a perfect correlation (anticorrelation) in the signs between the fluctuations among nearest neighbors if $\mathcal{P}=1$ ($\mathcal{P}=0$). Uncorrelated disorder is recovered for $\mathcal{P}=0.5$. In Fig. 5 the fidelity as a function of ε_J ($\varepsilon_B=0$) for different values of $\mathcal{P}$ is plotted. Notice that the fidelity decay is a monotonic function of $\mathcal{P}$. Anticorrelated disorder is more dangerous than correlated one.

Within the model of disorder studied in this work, strong fluctuations of the exchange couplings lead to a degradation of the signal while the same protocol is not very sensitive (especially for long chains) to fluctuations in the local magnetic fields.

IV. LEVEL SPACING STATISTICS

The behavior of the fidelity is essentially dictated by the time dependence of the amplitude f_N defined in Eq. (5). A deeper insight of its characteristics in disordered chains can be understood by analyzing the statistics of the level spacing of the spin-chain Hamiltonian in presence of disorder. The level spacing statistics $P(s)$ is widely used to study complex many-body systems [19] and quantum systems with classically chaotic counterparts [20] in the framework of random matrix theory [16]. The distribution $P(s)ds$ gives the probability that the energy difference between two adjacent levels (normalized to the average level spacing) belongs to the interval $[s, s+ds]$. The Hamiltonian (1) is a tridiagonal matrix
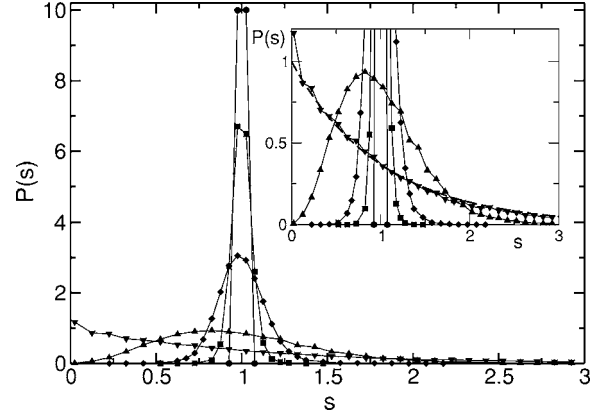
and thus it is not a random matrix, however, we will show that this analysis helps in understanding the behavior of the disordered chain. The level spacing statistics can still be used to characterize the crossover that static imperfections induce in the spectrum of the Hamiltonian.

The Hamiltonian H is a tridiagonal matrix with zero entries on the diagonal, and $H_{k,k+1}=H_{k+1,k}=\lambda\sqrt{k(N-k)}$ where N is the chain length and λ a constant. Without any perturbation ($\epsilon_J=\epsilon_B=0$) the energy levels are then equally spaced, while in presence of strong random perturbations ($|\epsilon_J|\sim1$) its eigenvalues are completely uncorrelated. This crossover is detected by the level spacing statistics. It changes from a delta function to a Poisson distribution given by the formula

$$P_D(s)=\delta(s-1) \quad \text{no disorder,} \tag{11}$$

$$P_P(s)=\exp(-s) \quad \text{strong disorder.} \tag{12}$$

Figure 6 shows this crossover: $P(s)$ changes from one limiting case to the other as a function of static imperfection strength. This crossover can be quantitatively characterized by the parameter

$$\eta=\frac{\displaystyle\int_0^1 |P(s)-P_P(s)|ds}{\displaystyle\int_0^1 |P_D(s)-P_P(s)|ds}, \tag{13}$$

which varies from $\eta=1$ in the case of a delta function to $\eta=0$ for a Poisson distribution [13]. In Fig. 7 we show the dependence of η on the strength of the perturbation. The crossover starts at $\epsilon_J\sim10^{-3}-10^{-2}$ depending on the length of the chain. In the inset of Fig. 7 we report the dependence of the imperfection strength η_c at which the parameter η reaches a given constant value ($\eta=0.5$, 0.8). The threshold η_c drops with the spin length as
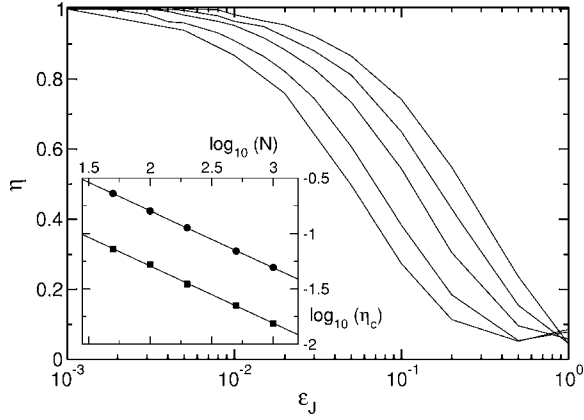
FIG. 7. The parameter η as a function of the strength of the static imperfections ϵ_J. Different curves correspond to different spin chain length: from right to left $N=50$, $N=100$, $N=200$, $N=500$. We averaged over N_{av} disorder realizations with $N_{av}=10^4$. Inset: scaling of the parameter η_c as a function of the chain length N obtained from the condition $\eta=0.5$ (circles) and $\eta=0.8$ (squares). Straight lines are proportional to $N^{-0.5}$.

$$\eta_c \sim N^{-0.5}.$$

Thus it follows the same law found in the previous section regarding the fidelity of the state transfer.

In the next section, we show that the same crossover is reflected by the fidelity time series with the appearance of a fractal behavior.

V. FRACTAL DIMENSION OF THE FIDELITY

An interesting consequence of the modification of the spectrum, and hence of the fidelity, in presence of static imperfections emerges in the time dependence of the fidelity. In this section we will not look for the optimal time for the state transfer but rather analyze its behavior as a function of time. It appears that the time signal of the fidelity has a fractal behavior. In order to measure the fractal dimension of the signal we used the modified box counting algorithm [21]. In the standard box counting algorithm the fractal dimension D of the signal is obtained by covering the data with a grid of square boxes of size L^2. The number $M(L)$ of boxes needed to cover the curve is recorded as a function of the box size L. The (fractal) dimension D of the curve is then defined as

$$D = -\lim_{L\to 0}\log_L M(L). \tag{14}$$

One finds $D=1$ for a straight line, while $D=2$ for a periodic curve. Indeed, for times much larger than the period, a periodic curve covers uniformly a rectangular region. Any given value of D in between of these integer values is a signal of the fractality of the curve. The modified algorithm of Ref. [21] follows the same lines but uses rectangular boxes of size $L\times\Delta_i$ (Δ_i is the largest excursion of the curve in the region L). Then, the number
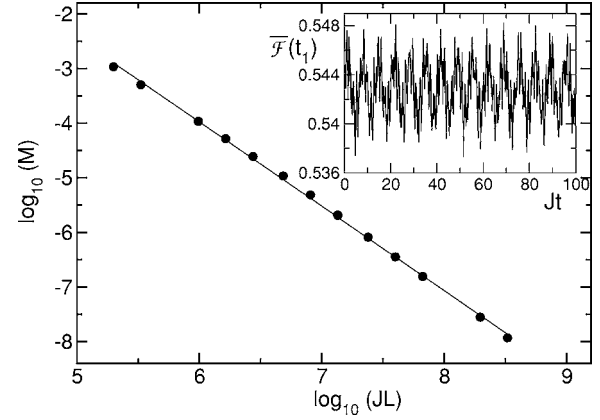

FIG. 8. M as a function of the interval JL. A numerical fit gives a fractal dimension $D=1.52$. Inset: Temporal evolution of the fidelity up to time $T=10^4/J$ in the presence of disorder for $\varepsilon_J=0.26$, $\varepsilon_B=0$, $N_{av}=1$, $N=500$.

$$M(L) = \frac{\sum_i \Delta_i}{L} \tag{15}$$

is computed (the time boxes L are expressed in units of the exchange coupling J). For any curve a region of box lengths $L_{min}<L<L_{max}$ exists where $M \propto L^D$. Outside this region one either finds $D=1$ or $D=2$: The first equality ($D=1$) holds for $L<L_{min}$ and it is due to the coarse grain artificially introduced by any numerical simulations. The second one ($D=2$) is obtained for $L>L_{max}$ and it is due to the finite length of the analyzed time series. The boundaries L_{min}, L_{max} have to be chosen properly for any time series.

We apply the modified algorithm to the signal of the fidelity for a single realization of disorder after a transient regime needed to reach the average value of $\mathcal{F}=0.5$: The inset of Fig. 8 shows the typical fluctuating signal we analyzed while Fig. 8 shows the numerically computed function $M(L)$ which gives a fractal dimension $D=1.52$. It is natural to investigate the dependence of the fractal dimension with the static imperfection strengths: the results of numerical simulations are given in Fig. 9. The curve changes gradually its dimension from $D\approx 2$ (periodic curve) to $D=1$ for very large imperfection strengths. This last result is due to the fact that for very large disorder the fidelity drops almost immediately to 0.5 corresponding to a complete loss of the initial state information: The fidelity remains then constant, characterized by dimension $D=1$. However, the most general situation in the presence of static imperfections is a fidelity with fractal dimension: defining, as before, a threshold of disorder strength D_c at which the fidelity has a given fractal dimension (between two and one), we find that this threshold drops as

$$D_c \sim N^{-0.5}.$$

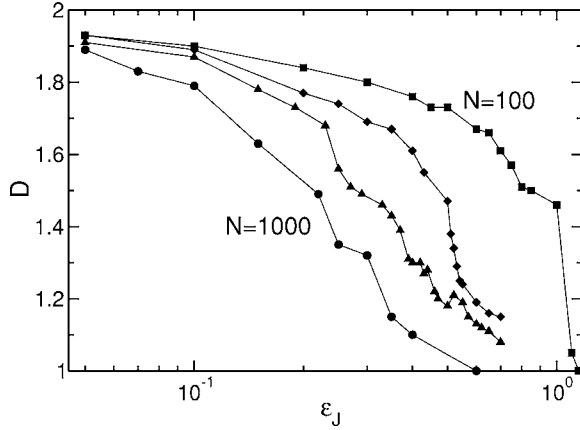This behavior is shown in Fig. 10 and follows exactly the same scaling as the parameters η_c and ϵ_J^c.

FIG. 9. Fractal dimension D of the signal $\mathcal{F}(t)$ as a function of the perturbation strength ε_J for $\varepsilon_B=0$, $N_{\text{av}}=1$ and, from right to left, $N=100$, $N=200$, $N=500$, $N=1000$. The error on the fractal dimension is of the order of 3%. For $\varepsilon_J<5\times10^{-2}$ the error on the fractal dimensions D increases significantly as $L_{\min}\lesssim L_{\max}$.

VI. CONCLUSIONS

We have shown that static imperfections in a modulated spin chain destroy, above a given threshold, the transmission of quantum states if performed following the protocols presented in Ref. [9]. We characterize the effects of static imperfections by means of the fidelity of the state transmission. This transition is reflected in the changing of the level spacing statistics (from delta correlated to completed uncorrelated) and in the behavior of the fidelity time series: the perfect state transfer is characterized by a periodic fidelity with integer fractal dimension while beyond the critical threshold it is described by a fractal dimension. We characterize these crossovers by analyzing ϵ_J^c, η_c, D_c: the imperfection strength needed to reach this value defines a critical threshold. The three distinct critical thresholds follow the same scaling as a function of the chain length and imperfection strength, independently from the critical value chosen. This common behavior reflects the profound changes in the quantum system induced by the presence of static imperfec-
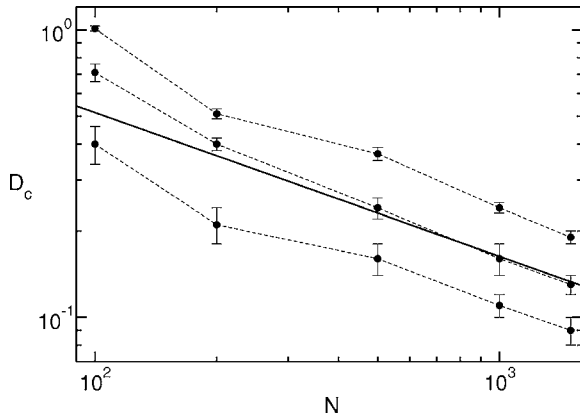

FIG. 10. Scaling parameter D_c as a function of chain length N from the condition $D=1.76$, 1.6, 1.4 (from bottom to the top) from Fig. 9. The full straight line is proportional to $N^{-0.5}$.

tions. The threshold drops as the square root of the chain length: this is a behavior similar to the one found in Ref. [14] in a different system where it was a consequence of the two-body nature of the interactions. Here, the dependence is mainly due to the fact that the system is confined to the subspace of one excitation. The conclusion of this analysis is that it is possible, at least in principle, to tolerate or correct the errors introduced by static imperfection.

APPENDIX: PERTURBATION THEORY

We are interested in evaluating the fidelity (7) averaged over different disorder realizations. Equation (6) shows that it depends on the matrix element

$$
\begin{aligned}
f_N(t) &= \langle N|e^{-\iota(H+H_I)t}|1\rangle \\
&= \langle N|e^{-\iota Ht}\mathcal{T}\left[\exp\left(-\iota\int_0^t dt\, e^{\iota Ht}H_I e^{-\iota Ht}\right)\right]|1\rangle \\
&= 1 + \mathcal{O}(H_I) + \mathcal{O}(H_I^2),
\end{aligned}
\tag{A1}
$$

where $\mathcal{T}$ is the time ordered product, $\hbar=1$, and H_I is the part of the Hamiltonian that describes the static imperfections b_k, δ_k. We first consider the case where $\delta_k=0$, that is, only random local magnetic fields are present. We develop the time-ordered product up to the second order in H_I. The first-order term reads

$$
\begin{aligned}
\mathcal{O}(H_I) &= -\iota\int_0^t dt\langle 1|e^{\iota Ht}H_I e^{-\iota Ht}|1\rangle \\
&= -\iota\sum_{\ell=1}^N b_\ell \int_0^t dt[1-2|U_\ell^1(t)|^2] \equiv -\iota\sum_{\ell=1}^N b_\ell C_\ell(t),
\end{aligned}
\tag{A2}
$$

where $U_\ell^k(t) \equiv \langle\ell|e^{-\iota Ht}|k\rangle$ [22]. The second order is given by

$$
\begin{aligned}
\mathcal{O}(H_I^2) &= -\int_0^t\int_0^t dt dt'\langle 1|e^{\iota Ht}H_I e^{-\iota H(t-t')}H_I e^{-\iota Ht'}|1\rangle \\
&= -\sum_{\ell=1}^N\sum_{m=1}^N b_\ell b_m\int_0^t\int_0^t dt\, dt'\left(1-2|U_m^1(t)|^2\right. \\
&\quad \left. -2|U_\ell^1(t')|^2 + 4U_m^{1*}(t)U_\ell^1(t')\sum_{k=1}^N U_m^k(t)U_k^{\ell*}(t')\right) \\
&\equiv -\sum_{\ell=1}^N\sum_{m=1}^N b_\ell b_m D_{\ell,m}(t).
\end{aligned}
\tag{A3}
$$

The fidelity (7) is given by the average over different disorder realization of the coefficient $f_N(t)$ and of its modulus square:

$$\overline{\mathcal{F}(t)} = \frac{1}{2} + \left\langle \frac{|f_N(t)|}{3} + \frac{|f_N(t)|^2}{6} \right\rangle_{\mathcal{D}}$$

$$\approx 1 - \frac{\varepsilon_B^2}{3} \sum_{k=1}^{N} \{2 \, \mathrm{Re}[D_{k,k}(t)] - C_k^2(t)\}/3. \qquad (A4)$$

The case for $\delta_k \neq 0$ is obtained following the same steps and with a final result of

$$\overline{\mathcal{F}(t)} = 1 - \frac{\varepsilon_B^2}{3} \sum_{k=1}^{N} \{2 \, \mathrm{Re}[D_{k,k}(t)] - C_k^2(t)\}/3$$

$$- \frac{\varepsilon_J^2}{3} \sum_{k=1}^{N} \{2 \, \mathrm{Re}[F_{k,k}(t)] - E_k^2(t)\}/3, \qquad (A5)$$

where the coefficients E_k, $F_{m,\ell}$ are given by

$$E_\ell = 4 \int_0^t dt \, \mathrm{Re}[U_\ell^1(t) U_{\ell+1}^{1*}(t)], \qquad (A6)$$

$$F_{m,\ell} = 4 \int_0^t \int_0^t dt \, dt' \sum_{k=1}^{N} [U_m^{1*}(t) U_k^{m+1}(t) + U_{m+1}^{1*}(t) U_k^m(t)]$$

$$\times [U_\ell^{1*}(t') U_k^{\ell+1*}(t') + U_{\ell+1}^{1*}(t') U_k^{\ell*}(t')].$$

The effects of the two different kinds of perturbations in Eq. (A5), the local magnetic b_ℓ fields and the couplings δ_k, are decoupled because they fluctuate independently from each other.

[1] N. Gisin, G. Ribordy, W. Tittel, and H. Zbinden, Rev. Mod. Phys. **74**, 145 (2002).

[2] C. H. Bennett, G. Brassard, C. Crépeau, R. Jozsa, A. Peres, and W. K. Wootters, Phys. Rev. Lett. **70**, 1895 (1993).

[3] L. Tian, P. Rabl, R. Blatt, and P. Zoller, Phys. Rev. Lett. **92**, 247902 (2004).

[4] S. Bose, Phys. Rev. Lett. **91**, 207901 (2003).

[5] V. Giovannetti and R. Fazio, Phys. Rev. A **71**, 032314 (2005).

[6] Y. Li, T. Shi, B. Chen, Z. Song, and C. P. Sun, Phys. Rev. A **71**, 022301 (2005).

[7] A. Romito, R. Fazio, and C. Bruder, Phys. Rev. B **71**, 100501(R) (2005).

[8] M. Paternostro, G. M. Palma, M. S. Kim, and G. Falci, Phys. Rev. A **71**, 042311 (2005).

[9] M. Christandl, N. Datta, A. Ekert, and A. J. Landahl, Phys. Rev. Lett. **92**, 187902 (2004).

[10] F. Verstraete, M. A. Martín-Delgado, and J. I. Cirac, Phys. Rev. Lett. **92**, 087201 (2004).

[11] T. J. Osborne and N. Linden, Phys. Rev. A **69**, 052315 (2004).

[12] D. Burgarth and S. Bose, Phys. Rev. A **71**, 052315 (2005); D. Burgarth, V. Giovannetti, and S. Bose, quant-ph/0410175.

[13] B. Georgeot and D. L. Shepelyansky, Phys. Rev. E **62**, 6366 (2000).

[14] G. Benenti, G. Casati, S. Montangero, and D. L. Shepelyansky, Phys. Rev. Lett. **87**, 227901 (2001).

[15] J. Zhang, G. L. Long, W. Zhang, Z. Deng, W. Liu, and Z. Lu, quant-ph/0503199.

[16] T. Guhr, A. Müller-Groeling, and H. A. Weidenmüller, Phys. Rep. **299**, 190 (1998).

[17] M. V. Berry, J. Phys. A **29**, 6617 (1996).

[18] E. J. Amanatidis, D. E. Katsanos, and S. N. Evangelou, Phys. Rev. B **69**, 195107 (2004).

[19] F. Haake, *Quantum Signature of Chaos* (Springer-Verlag, New York, 1991).

[20] F. Izrailev, Phys. Rep. **196**, 299 (1990).

[21] A. S. Sachrajda, R. Ketzmerick, C. Gould, Y. Feng, P. J. Kelly, A. Delage, and Z. Wasilewski, Phys. Rev. Lett. **80**, 1948 (1998).

[22] The matrix elements $U_\ell^k(t)$ are well known, and can be found in R. P. Feynman, R. B. Leighton, and M. Sands, *Feynman Lectures on Physics* (Addison-Wesley, Reading, MA, 1965), Vol. 3.